Atmospheric Research 183 (2017) 42–57

Contents lists available at ScienceDirect

Atmospheric Research

journal homepage: www.elsevier.com/locate/atmosres

A multi-sensor study of the impact of ground-based glaciogenic seeding on clouds and precipitation over mountains in Wyoming. Part II: Seeding impact analysis

Binod Pokharel [a,*], Bart Geerts [a], Xiaoqin Jing [a], Katja Friedrich [b], Kyoko Ikeda [c], Roy Rasmussen [c]

[a] Department of Atmospheric Science, University of Wyoming, Laramie, WY 82071, USA
[b] Department of Atmospheric and Oceanic Sciences, University of Colorado, Boulder, CO 80309, USA
[c] Research Application Laboratory, National Center for Atmospheric Research, Boulder, CO 80307, USA

ARTICLE INFO

Article history:
Received 4 May 2016
Received in revised form 10 August 2016
Accepted 20 August 2016
Available online 23 August 2016

Keywords:
Glaciogenic seeding
Orographic cloud and precipitation
Radar reflectivity
Airborne measurements

ABSTRACT

The AgI Seeding Cloud Impact Investigation (ASCII) campaign, conducted in early 2012 and 2013 over two mountain ranges in southern Wyoming, was designed to examine the impact of ground-based glaciogenic seeding on snow growth in winter orographic clouds. Part I of this study (Pokharel and Geerts, 2016) describes the project design, instrumentation, as well as the ambient atmospheric conditions and macrophysical and microphysical properties of the clouds sampled in ASCII. This paper (Part II) explores how the silver iodide (AgI) seeding affects snow growth in these orographic clouds in up to 27 intensive operation periods (IOPs), depending on the instrument used.

In most cases, 2 h without seeding (NOSEED) were followed by 2 h of seeding (SEED). In situ data at flight level (2D-probes) indicate higher concentrations of small snow particles during SEED in convective clouds. The double difference of radar reflectivity Z (SEED − NOSEED in the target region, compared to the same trend in the control region) indicates an increase in Z for the composite of ASCII cases, over either mountain range, and for any of the three radar systems (WCR, MRR, and DOW), each with their own control and target regions, and for an array of snow gauges. But this double difference varies significantly from case to case, which is attributed to uncertainties related to sampling representativeness and to differences in natural trends between control and target regions. We conclude that a sample much larger than ASCII's sample is needed for clear observational evidence regarding the sensitivity of seeding efficacy to atmospheric and cloud conditions.

1. Introduction

This is the second part of an observational study that explores whether a measurable signal of ground-based glaciogenic seeding can be detected, in terms of ice crystal size distribution and mainly snowfall rate. Pokharel and Geerts (2016, hereafter referred to as Part I) describes the AgI Seeding Cloud Impact Investigation (ASCII) experimental design, as well as the characteristics of the sampled orographic clouds, flow field, and upstream stability profiles in ASCII's 27 intensive operation periods (IOPs). A map of the terrain, the facilities deployed in ASCII, and the flight track of the University of Wyoming King Air (UWKA) is shown in Fig. 1. This paper (Part II) compares particle size distributions, precipitation rates, and mainly radar reflectivity profiles for all these IOPs. Comparison are drawn both spatially (target vs. control regions) and temporally (SEED vs. NOSEED).

Comparisons using three different radar systems are described in Section 2, and comparisons based on particle probe data are made in Section 3. The impact of seeding is estimated in Section 4, using double differences based on these radar systems as well as snow gauges. Caveats and suggestions for improvements are discussed in Section 5. The findings are summarized in Section 6.

2. Change in radar reflectivity

This section examines the change in reflectivity from NOSEED to SEED periods for three different radar systems, each with their own target and control regions. These are the W-band (3 mm) airborne profiling Wyoming Cloud Radar (WCR), the volume-scanning X-band (3 cm) Doppler on Wheels (DOW) radar, and a pair of profiling Ka-band (1.2 cm) Micro Rain Radars (MRRs), all described in Part I. We start with composite reflectivity profiles from the WCR, based on all available ASCII IOPs, listed in Table 1 in Part I. First we define the control region as the flight leg upwind of the AgI generators (leg 1 in Fig. 1) and the target

Abbreviations: ZIP, reflectivity impact factor; PIF, precipitation impact factor; ASCII, AgI Seeding Cloud Impact Investigation; UWKA, University of Wyoming King Air; WCR, Wyoming Cloud Radar; WCL, Wyoming Cloud Lidar; MRR, Micro-Rain Radar; DOW, Doppler on Wheels.

* Corresponding author at: Department of Atmospheric Science, University of Wyoming, Laramie, WY 82072, USA.
E-mail address: bpokhare@uwyo.edu (B. Pokharel).

http://dx.doi.org/10.1016/j.atmosres.2016.08.018
0169-8095/

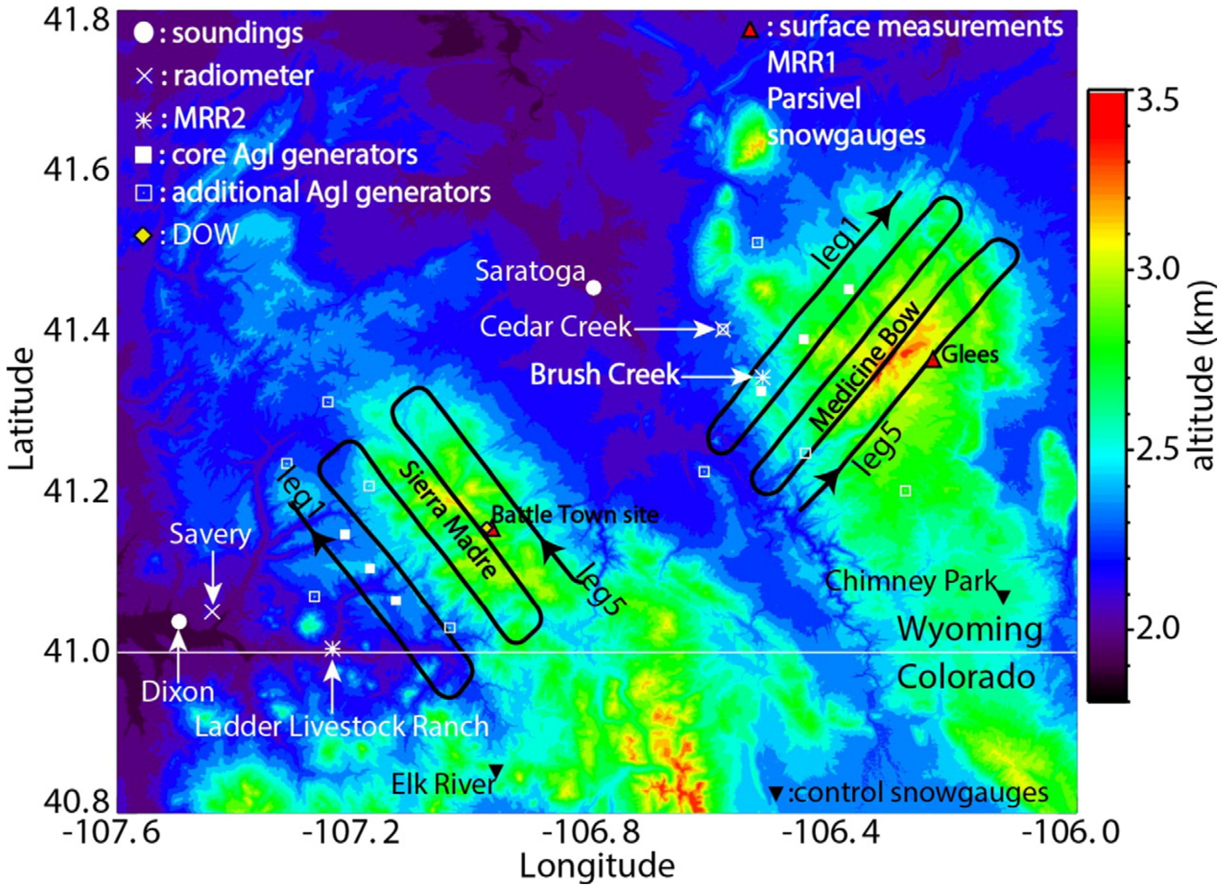

Fig. 1. Terrain map and ASCII deployment map over the Sierra Madre (SM) and Medicine Bow (MB) Mountains in southern Wyoming. The solid black lines show the fixed UWKA flight tracks and square symbols show the ground-based AgI generators. The three most commonly used AgI generators are shown by the filled squares.

region as the four downstream legs (Section 2.1). Next, to build evidence that differences are seeding-related, we contrast temporal changes inside dispersion plumes (target) against those outside (control) (Section 2.2). We also contrast Medicine Bow (MB) vs. Sierra Madre (SM) (Section 2.3), and convective vs. stratiform clouds (Section 2.4). Finally, we evaluate the reflectivity changes from NOSEED to SEED for the MRR pair (Section 2.5) and for the DOW (Section 2.6).

2.1. Target and control WCR reflectivity

A seeding signature is not immediately obvious in the reflectivity pattern downwind of AgI generators in any IOP. Therefore the WCR reflectivity profiles are composited for all flight legs in the form of frequency-by-altitude displays (FADs) (Yuter and Houze, 1995). The frequency is normalized, such that any number of transects can be added, and the sum of all counts (all heights, all reflectivity bins) equals 100%. The height is expressed above ground level (AGL) because AgI seeding is ground-based and, to a first order, low-level tracers are advected over the terrain, roughly following the terrain contour. The FAD approach has been used in several ASCII case studies (Pokharel et al., 2014a, 2014b, 2015). Here we use it for the composite of all available cases: the WCR reflectivity FAD for 21 ASCII IOPs is shown in Fig. 2. This includes nine IOPs over the SM and 12 IOPs over the MB. Three IOPs in pre-ASCII (10, 25 and 30 March 2009) are excluded because no control measurements were collected (Table 1 in Part I).

WCR reflectivity data from the target tracks (legs 2–5) and the control track (leg 1) are composited during NOSEED and SEED (Fig. 2). In most IOPs NOSEED preceded SEED, enabling a rapid transition between the two periods, although the UWKA flew one or two cross-mountain along-wind legs between the two periods (*e.g.*, Fig. 4 in Part I), to allow AgI nuclei to disperse. Both periods usually contain two full ladders of five legs (Fig. 1), and thus the WCR sample size of SEED is about the same as that of NOSEED. As can be seen in the cumulative distance listed in the upper four panels of Fig. 2, the SEED sample size is 15–20% smaller on average than the NOSEED sample size in both regions. This is because in some IOPs the aircraft was unable to complete the 4th ladder (part of SEED), and in some cases the wind was not strong enough for the first leg flown on ladder 3 (leg 5, furthest downwind, Fig. 1) to be counted as part of SEED. The exact start and end times for NOSEED and SEED are listed in Table 1 in Part I.

The dip in the “data presence” line between 1 and 2 km AGL in all upper four panels in Fig. 2 is an artifact due to the radar blind zone (*e.g.*, Fig. 4 in Part I). It gives an indication of the typical flight level AGL. The average reflectivity is computed in Z units ($\mathrm{mm^6\ m^{-3}}$) and expressed in dBZ in Fig. 2. It is converted to precipitation rate R ($\mathrm{mm\ h^{-1}}$) in the upper abscissa of the two lower panels of Fig. 2 using:

$$R = aZ^b \tag{1}$$

For the WCR we use $a = 0.39$, and $b = 0.58$ in Eq. (1), based on Pokharel and Vali (2011), who use WCR data collected over and near the MB range. This is close to the Z–R relationship derived theoretically for mm-wavelength radar by Matrosov (2007). The uncertainty in these relationships is large (larger than factor of two), mainly because of the uncertainty in ice particle density, which is strongly affected by riming. For the MRR and the DOW radars, we use $a = 0.046$, and $b = 0.67$ in Eq. (1), based on Matrosov et al. (2009). The precipitation rate in Fig. 2 is a conditional rate, *i.e.* when it is snowing. The fraction of time it was snowing at any height can be estimated from the data presence line.